GLOBAL BIOGEOCHEMICAL CYCLES, VOL. 14, NO. 4, PAGES 1123-1136, DECEMBER 2000

Simulating the effects of climate change and climate variability on carbon dynamics in Arctic tundra

Marc Stieglitz
Lamont-Doherty Earth Observatory, Columbia University, Palisades, New York

Anne Giblin, John Hobbie, and Mathew Williams
Marine Biological Laboratory, The Ecosystems Center, Woods Hole, Massachusetts

George Kling
Department of Biology, University of Michigan, Ann Arbor

Abstract. Through a simple modeling exercise, three mechanisms have been identified, each operating at a different timescale, that may govern carbon dynamics in Arctic tundra regions and partially explain observed CO_2 flux variability. At short timescales the biosphere reacts to meteorological forcing. Drier conditions are associated with aerobic soil decomposition, a large CO_2 efflux, and a net ecosystem loss of carbon. Cooler and moister conditions favor slower anaerobic decomposition in soils, good growing conditions, and terrestrial carbon sequestration. At intermediate timescales, periods of terrestrial carbon loss are directly linked to periods of carbon sequestration by the ability of the ecosystem to retain labile nitrogen. Labile nitrogen released to the soil during periods when the tundra is a source of carbon (soil respiration > net primary productivity) is retained within the ecosystem and accessed during periods when carbon sequestration is favored (net primary productivity > soil respiration). Finally, the ability of vegetation to respond to long-term changes in soil nutrient status via changes in leaf nitrogen and leaf area index modulates this dynamic at intermediate to long timescales.

1. Introduction

Northern soils hold ~ 30% of the world's soil organic carbon [*Post et al.*, 1982]; between 43 and 200 gigatons of this is in tundra soils [*Post et al.*, 1982; *Shaver et al.*, 1992] and 200-500 gigatons is in boreal forests [*Dixon et al.*, 1994; *Gorham*, 1991; *Schlesinger*, 1977; *Whittaker*, 1975]. While climatic conditions may have been favorable for carbon sequestration during the past 10,000 years in arctic regions [*Billings*, 1987; *Gorham*, 1991; *Oechel and Billings*, 1992], this may no longer be the case. High northern latitudes have warmed ~1°-2°C during the past century [*Beltrami and Mareschal*, 1991; *Chapman and Walsh*, 1993; *Garfinkel and Brubaker*, 1980; *Jacoby and Darrigo*, 1995; *Kakuta*, 1992; *Lachenbruch and Marshall*, 1986; *Overpeck and al.*, 1997], and warming is expected to continue into the next century [*Houghton et al.*, 1995]. What will be the fate of arctic peatlands in a warmer world? If soils become warmer, increased microbial activity may release carbon stored in the soil. At the same time, increased temperatures may also augment plant growth and thus sequester atmospheric CO_2. Which of these two processes dominates will determine whether tundra biomes are a net source or net sink of atmospheric CO_2 in a climate-changed world. To answer these questions for the entire Arctic, we need a new generation of models that are physically based, computationally efficient, and can operate at the scales required by today's regional and global climate models. In addition these models will need to integrate hydrologic, thermal, and biologic processes within a coherent framework. We have developed a detailed hydrologic model that includes topographic effects, soil freeze-thaw processes, and snow physics. The model is capable of operating in permafrost environments [*Stieglitz et al.*, 1999] and is coupled with a simple biological model that includes soil microbial processes and above ground net primary productivity. We use this model to explore the mechanisms that control CO_2 flux variability and, ultimately, net carbon sequestration in a warmer world. Further, we explore the hypothesis that on short-to-intermediate timescales, variability in ecosystem fluxes can be explained by the interaction between climate variability and the ability of the ecosystem to retain labile nitrogen (nitrogen in readily usable forms).

Paper number 1999GB001214.
0886-6236/00/1999GB001214$12.00

2. Background

Measured tundra CO_2 fluxes over the last 25 years have been quite variable. Growing season measurements in the 1970s indicated that tundra biomes in northern Alaska were accumulating carbon (acting as an atmospheric carbon sink) at the rate of ~ 25 g C m^{-2} yr^{-1} for moist tussock tundra and 70 g C m^{-2} yr^{-1} for coastal wet sedge [*Chapin et al.*, 1980; *Coyne and Kelley*, 1975; *Miller et al.*, 1983; *Oechel et al.*, 1995]. From the middle 1980s through the early 1990s, measurements suggested these same biomes were losing carbon to the atmosphere (acting as an atmospheric carbon source) [*Oechel et al.*, 1995, 1993, 1997; *Vourlitis and Oechel*,

1997, 1999; *Zimov et al.*, 1996, 1993]. For example, from 1983 to 1993, moist tussock tundra at Toolik Lake and Happy Valley, Alaska, lost carbon at an average rate of ~144 g C m^{-2} yr^{-1}during the growing season [*Vourlitis and Oechel*, 1999]. Likewise, over a 3-year period beginning September 1989 at a forest tundra site in the Russian North, *Zimov et al.* [1996] found the net summer efflux of CO_2 ranged between 75 and 175 g C m^{-2} yr^{-1}. However, the most recent growing season measurements indicate that tundra regions may once again be sequestering atmospheric carbon. Eddy covariance and chamber measurements (1994 - 1996) along a transect from Toolik Lake to Prudhoe Bay, Alaska, showed wet sedge and moist tussock tundra to be a gaining carbon at a rate of 10 g C m^{-2} yr^{-1} and 50 g C m^{-2} yr^{-1}, respectively [*Vourlitis and Oechel*, 1999; *Vourlitis et al.*, 1998].

For our analysis we focus on measurements made during the growing season, typically the 120-day period from June through August. These were the only measurements made for much of these three decades as it was presumed that the frozen winter soils were biologically inactive. However, it has now been determined that winter respiration comprises a significant fraction of the total annual soil efflux of CO_2 in some arctic environments [*Oechel et al.*, 1997; *Zimov et al.*, 1996, 1993]. None the less, growing season measurements indicate that year-to-year and decade-to-decade variability in the source/sink activity of the Arctic is quite large.

How can this variability in land-atmosphere CO_2 fluxes be explained? *Vourlitis and Oechel* [1999] hypothesize that after the relatively warm and dry 1980s, when the terrestrial biome was losing carbon to the atmosphere, there was an acclimation of community composition and plant physiology such that a return to carbon sequestration was possible. In this work we demonstrate that the degree to which the ecosystem can respond to changing soil nutrient conditions may play a significant role in governing the variability in ecosystem fluxes at intermediate to long timescales. Specifically, periods of terrestrial carbon loss are directly linked to periods of carbon sequestration through the ability of the ecosystem to retain labile nitrogen. Nitrogen released to the soil during periods of carbon source activity (soil respiration > net primary productivity) is retained within the ecosystem and accessed during periods that favor carbon sink activity (net primary productivity > soil respiration).

3. The Imnavait Creek Catchment

This section summarizes extensive research on the Imnavait Creek catchment described by *Hinzman et al.* [1996, 1991], *Kane et al.* [1991], and *McNamara et al.* [1997]. The Kuparuk River (the basin is 8140 km^2) has its headwaters in the Brooks Range and drains through the foothills and coastal plain of northern Alaska to the Arctic Ocean. The Imnavait Creek subcatchment (2.2 km^2) lies within the headwaters of the Kuparuk Basin at 68°N. Imnavait Creek is located in rolling piedmont hills, where the predominant soils are 15-20 cm of porous organic peat underlain by silt and glacial till [*Hinzman et al.*, 1991]. The topographic sequence of land cover ranges from wet sedge in the riparian zones to tussock tundra along the midslopes to dry heath near the ridge tops. Water tracks, regions of enhanced soil moisture that run down the hillslope at a spacing of ~10 m, channel flow down the slope. From 1985 through 1993 the mean annual precipitation, maximum snow water equivalent, and air temperature averaged 34 cm, 12 cm, and -7.4°C, respectively; 66% of the annual precipitation fell during the short summer season. Snowmelt accounted for 47% of annual discharge while runoff and evapotranspiration were 46 and 54% of the water budget, respectively. Snowfall is possible throughout the year; however, the snow season begins in earnest in September when soil freezing begins. Spring melt is in late May or early June. The maximum thaw depth in summer ranges from 25 to 100 cm depending on vegetation, aspect, slope, and soils. Hydrologic activity is limited to the near surface because of the shallow maximum thaw depth and the fact that saturated hydrologic conductivities fall off extremely rapidly below the porous organic layer.

4. Data Sets

In combination with digital elevation data at a resolution of 20 x 20 m, two meteorological data sets are used to force the land surface model. The first comprises 2.5 years of hourly meteorological and hydrological data taken at Imnavait Creek between May 1991 and October 1993. Discharge and ground temperature measurements taken during this period are used for validation (provided by D. Kane and L. Hinzman, University of Alaska). The second is a 160-year hourly data set constructed from hourly meteorological data taken at Imnavait Creek during 1992 and monthly general circulation model (GCM) output fields.

A number of GCMs have been used to conduct global warming experiments spanning the period 1860-2100 [*Houghton et al.*, 1995]. In general, these experiments include a control integration experiment and a warming experiment. The control integration experiment uses present-day CO_2 concentrations to evaluate the ability of the model to simulate today's climate and to determine the stability of the climate generated, i.e., to determine if the climate drifts as it evolves. The warming experiments use an effective greenhouse forcing corresponding to that observed from 1900 to 1990 and a forcing thereafter which corresponds to an increase of CO_2 of 1% yr^{-1}. In this scenario, CO_2 concentrations double between 1990 and 2060. We use simulations from the Canadian Climate Centre (CCC) coupled GCM which include sulfate aerosols. The CCC simulations are chosen because (1) the control integration and the transient simulation for the 1990s both produce a fairly realistic arctic climate and (2) the warming associated with the 1990-2060 period is representative of most GCM simulations. While some GCM simulations do produce slightly more warming, the drying effect of enhanced warming is offset by enhanced precipitation.

As stated, the 160-year hourly forcing data set is constructed from a composite of the hourly meteorological data taken at Imnavait Creek in 1992 and monthly output fields from the 1900 - 2060 transient warming simulation at the grid cell that encompasses Imnavait Creek. Using precipitation as an example, the constructed field for a given hour, Julian date, and year is derived by dividing the hourly site data by its corresponding monthly mean and multiplying this quantity by the monthly GCM field for that year. The bias that exists between data taken at Imnavait Creek in 1992 and the CCC simulation data for the early 1990s is accounted for. This bias is assumed to be constant throughout the 160-year period.

5. Modeling

5.1. Hydrologic Cycle

The tundra landscape is unique. Infiltration and soil water movement is confined to shallow zones by permafrost, and the seasonal regimes of rivers, soil moisture, and surface-groundwater

interactions are dominated by freeze-thaw processes. In contrast to the temperate regions, these shallow zones limit the base flow that is typically supplied by deeper groundwater in other areas; thus surface runoff, which ceases soon after the precipitation event ends, is the dominant discharge mechanism [*Haugen et al.*, 1982; *McNamara et al.*, 1998]. Further, until the active layers deepen into mineral soils, much of the soil water flows through a narrow zone in contact with plant roots and soil organic matter.

The unique capacity of organic peat soils to retain water further limits the generation of base flow. While typical soils have porosities ranging from 40 to 50% and field capacities ranging from 10 to 40% by volume, peat soils of the North Slope of Alaska may have porosities above 90% and field capacities between 60 and 70% [*Hinzman et al.*, 1991]. Therefore peat soils cannot only hold large quantities of water (due to high porosities) but will also retain large quantities of water (due to high field capacities). Significant base flow occurs only when the soil moisture is relatively high, of the order of the field capacity. Finally, the restriction of hydrologic activity to the organic zone greatly influences the fluxes of CO_2 between the terrestrial landscape and the atmosphere.

We combine two methods of modeling the flow of water within a catchment. The first makes use of a soil column framework traditionally employed in most GCMs which simulate the vertical movement of water and heat within the soil and between the soil surface plus vegetation to the atmosphere. The second method makes use of the statistics of the topography and allows us to track the horizontal movement of shallow groundwater from the uplands to the lowlands (a TOPMODEL or topographic approach [*Beven et al.*, 1994; *Beven*, 1986a, b; *Beven and Kirkby*, 1979]). TOPMODEL formulations make use of knowledge of the mean depth of the water table and a probability density function (pdf) for soil moisture deficit (derived from topographic statistics) to permit dynamically consistent calculations of both the saturated fraction of the watershed (partial contributing area) and the base flow which supports this area. By combining these two approaches, we can produce a three-dimensional picture of soil moisture distribution within a catchment without the need to explicitly model the landscape. Since the approach relies only on the statistics of the topography, rather than the details of the topography, it is computationally inexpensive and compatible with the large spatial scales of today's climate models.

The approach taken follows *Stieglitz et al.* [1997]. We incorporate the analytic form of the TOPMODEL equations with a single column land surface model that tracks the mean state of the catchment variables. The ground scheme consists of 10 soil layers. Diffusion and a modified tipping bucket model govern heat and water flow, respectively. The prognostic variables, heat and water content, are updated each time step. In turn, the fraction of ice and temperature of a layer may be determined from these vari-

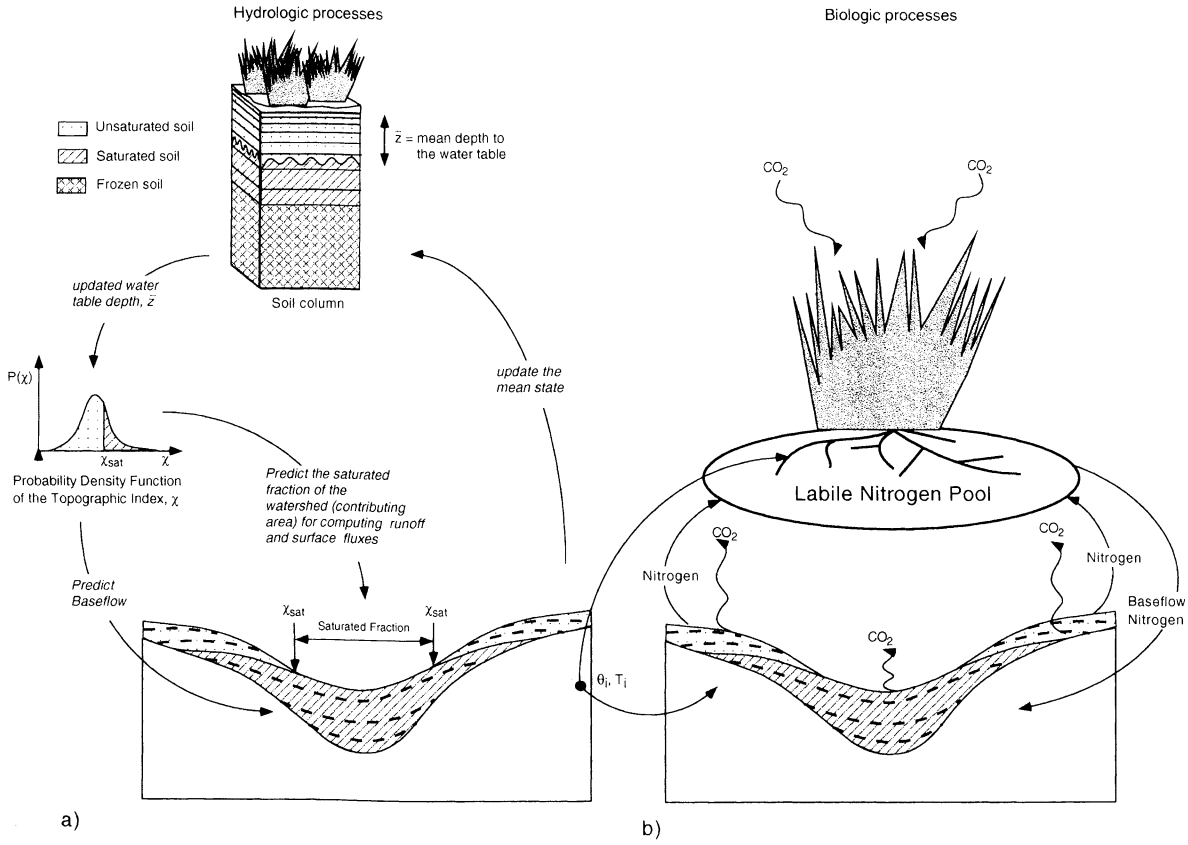

Figure 1. Integration of hydrologic, thermal, and biologic processes. (a) Hydrologic and thermal processes: TOPMODEL equations and digital elevation data are used to generate base flow and the associated saturated fraction. (b) Biologic processes: Model generated soil temperatures and soil moisture content drive soil respiration. Meteorological conditions, model generated soil moisture content, and soil nutrient status drive NPP.

ables. A three-layer snow model [*Lynch-Stieglitz*, 1994] and a modified BEST vegetation scheme [*Pitman et al.*, 1991] have been incorporated into the model framework. Radiation and atmospheric conditions determine the surface energy balance. TOPMODEL equations and digital elevation model (DEM) data are used to generate base flow, which supports lowland saturated zones. Soil moisture heterogeneity represented by saturated lowlands (predicted by TOPMODEL equations) subsequently impacts catchment evapotranspiration, the partitioning of surface fluxes, and the development of the storm hydrograph. Figure 1a depicts the current application of TOPMODEL equations. This approach to modeling the land surface has been validated at several catchments; these range in scale from the Red Arkansas Basin (570,000 km^2 [*Ducharne et al.*, 2000], to the Sleepers River catchment (Vermont, 8.4 km^2 [*Stieglitz et al.*, 1997]), to the Imnavait Creek catchment (2.2 km^2 [*Stieglitz et al.*, 1999]). As shown in Figure 1a and 1b, and discussed in section 5.2, the thermal and soil moisture status generated from the hydrologic model is used to drive biological processes, specifically net primary productivity (NPP) and soil respiration.

5.2. Carbon and Nitrogen Cycle

5.2.1. Carbon sequestration: NPP. The Aggregated Canopy Model (ACM) [*Williams et al.*, 1997] is a simple, highly aggregated model that simulates terrestrial gross primary productivity (GPP) in diverse environments and ecosystems. The starting point was a fine-scale, multilayer model of half-hourly vascular plant processes [*Williams et al.*, 1996], originally parameterized for and tested against CO_2 flux data from Harvard Forest, Massachusetts. More recently, this model has been modified for Arctic ecosystems. Over varied growing season conditions, this fine-scale model simulated hourly net carbon fluxes that were in good agreement with independent data from eddy covariance studies collected at nine sites (including shrub, tussock, and wet sedge tundra) across northern Alaska [*Williams et al.*, 2000]. Using a heuristic process, a simple aggregated set of equations operating on cumulative or average values (daily) of the most sensitive driving variables (leaf area index, mean foliar nitrogen concentration, daily maximum and minimum temperature, atmospheric transmittance, latitude, day of year, and an index of soil moisture) were derived. The aggregated model was calibrated to provide estimates of GPP similar to those of the fine-scale model across a wide range of these driving variables. The calibration across this broad range of conditions captured 96% of fine-scale model behavior but was computationally 3 orders of magnitude faster. For this application, we assumed that the daily NPP is one half of daily GPP. The resulting NPP calculated from the model is consistent with NPP determined from biomass harvests at the Toolik Lake Long Term Ecological Research (LTER) station [*Chapin and Shaver*, 1996; *Chapin et al.*, 1995]. Further, we assume that modeled soil respiration pertains only to the decomposition of organic matter and does not include root respiration. Root respiration is reflected in the difference between GPP and NPP.

In this study, ACM is forced with meteorological data and hydrologic model-generated soil moisture. Two key biotic parameters, leaf area index (LAI) and total foliar nitrogen must be specified. LAI determines the capacity of vegetation to intercept photosynthetically active radiation and thus controls the rates of photosynthetic light reactions. Foliar nitrogen concentration is strongly correlated with the concentration of key enzymes involved in light reactions (chlorophyll, light harvesting complexes) and dark reactions (Rubisco) and is thus a good proxy for the maximum rate of the photosynthetic metabolism [*Field and Mooney*, 1986]. In vascular plant communities across northern Alaska, there is a strong positive correlation between these variables among all the major physiographic vegetation types, from barrens to riparian shrubs [*Williams and Rastetter*, 1999]. Specifically, field surveys on the North Slope of Alaska indicate a highly positive correlation between the foliage light absorbing area and the photosynthetic capacity of vegetation (proportional to foliar nitrogen) [*Williams and Rastetter*, 1999]. This relationship simplifies the parameter requirements for ACM in arctic ecosystems as total foliar nitrogen (g N (m^2 ground area)$^{-1}$) can be estimated from LAI using the relationship derived by *Williams and Rastetter* [1999]: $N = 0.31 + 1.29\ LAI$ (n=14, $r^2 = 0.93$).

5.2.2. Carbon liberation: Soil decomposition. In saturated zones along creeks, where decomposition takes place under anoxic conditions, microbial respiration is relatively slow; in unsaturated uplands, decomposition is likely to be aerobic and microbial

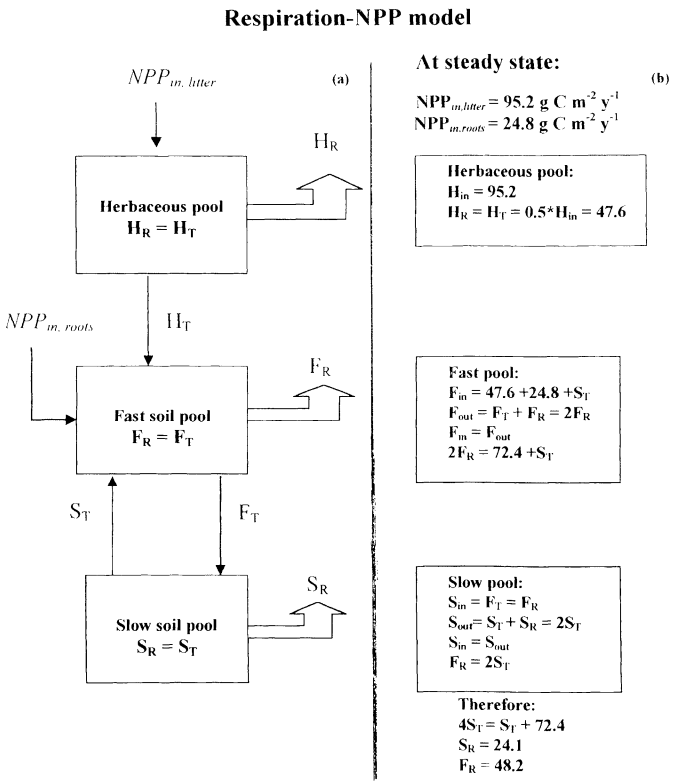

Figure 2. (a) Plant-soil carbon flux model. Thin arrows show biomass flows; thick arrows represent the soil respiration flux of CO_2 to the atmosphere. We assume that 50% of decomposed organic carbon is respired to the atmosphere as CO_2. (b) The 1900 – 1940 steady state calculation of annual soil fluxes. This assumes that annual NPP equals 120 g C m^{-2} yr^{-1} and NEP equals zero over the period. Pools are as follows: H, herbaceous pool; F, fast soil pool; S, slow soil pool. Subscripts are as follows: in, input of organic carbon to a pool; out, output of organic carbon from a pool; R, carbon loss to the atmosphere through microbial respiration (as CO_2); T, carbon transfer between the three pools.

respiration thus much faster. These aerobic/anaerobic zones are easily quantified using TOPMODEL and are identified in Figures 1a and 1b.

Three soil carbon pools are assumed; a herbaceous litter pool, a fast pool (rapid decomposition), and a recalcitrant pool (slow decomposition). Soil pool interactions are shown in Figure 2a. Microbial decomposition of material in one pool results in the liberation of CO_2 to the atmosphere due to respiration, with the remainder of the material transported from the source pool to a receiving pool. At the beginning of each time step the three pools are distributed within the soil column according to Figure 3a. The herbaceous carbon pool, considered to be leaf litter, is concentrated solely in model layer 1. The carbon concentration in the fast pool decays exponentially with depth, while the slow pool carbon concentration is constant with depth. We write the decomposition equation as

$$\text{decomposition (kg m}^{-2}\text{ s}^{-1}) = K(\text{Org})\,T_f(T)M_f(\theta), \qquad (1)$$

where K is the decomposition rate constant (s^{-1}), Org is amount of organic matter kg m^{-2}, T_f is the temperature function, and M_f is the soil moisture function. The temperature and soil moisture functions shown in Figure 3b follow *Waelbroeck and Louis* [1995] and *McKane et al.* [1997a]. Above the optimal soil moisture, 0.21 cm^3 cm^{-3}, decomposition proceeds asymptotically toward its anaerobic value of 15% of the optimal value. At moisture values less than 0.21 cm^3 cm^{-3}, the decomposition is inhibited by soil drying. Referenced to model layers this equation becomes

$$\text{decomposition}(_{i,j}) = K_j(\text{Org})_{i,j}T_f(T_{m,i})\left[M_f(\phi)f_{\text{sat}} + M_f(\theta_{u,i})(1 - f_{\text{sat}})\right], \qquad (2)$$

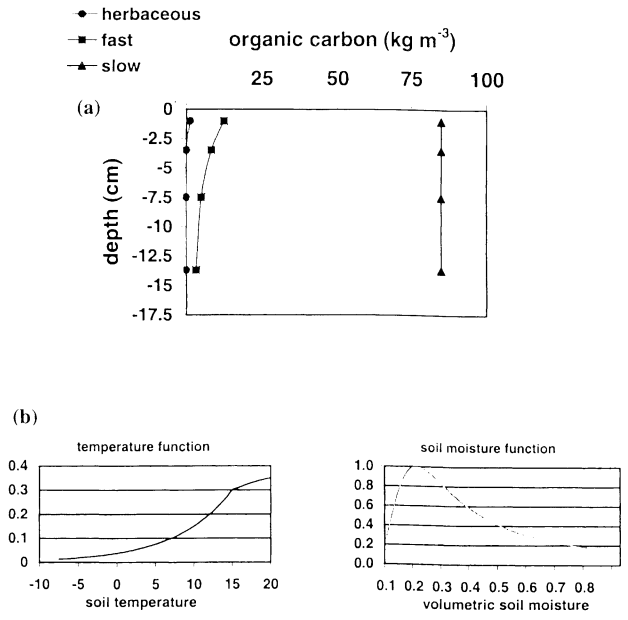

Figure 3. (a) Initial distribution of soil organic carbon among the first four model layers. The initial C stocks were assumed to be herbaceous pool, 25 g C m^{-2}; fast pool, 1000 g C m^{-2}; slow pool, 15000 g C m^{-2}. (b) Temperature and soil moisture functions (unitless) used in soil decomposition equation (2).

where i is the model layer, j is the soil pool, $T_{m,i}$ is the mean catchment soil temperature in model layer i, $\theta_{u,i}$ is the upland volumetric soil moisture in model layer i, ϕ is the saturated soil porosity (0.85 cm^3 cm^{-3} in peats), and f_{sat} is the saturated fraction of the catchment. The last two terms in (2) account for the effects of the dynamic expansion and contraction of lowland saturated zones. When upland recharge is large, base flow increases, lowland saturated zones expand, and the anaerobic term, $M_f(\phi)f_{\text{sat}}$, is significant. When recharge is small, base flow decreases, lowland saturated zones contract, and the aerobic term, $M_f(\theta_{u,i})(1\text{-}f_{\text{sat}})$, is dominant. Finally, the total soil column CO_2 production is simply the summed respiration for each of the organic pools in each of the soil layers.

Although only $T_{m,i}$, the mean catchment soil temperature in model layer i, is used in (2), the overall impact on model results of neglecting spatial variability in temperature should be small. In this relatively cold catchment, with a small elevation gradient of less than 40 m, upland-lowland variations in ground temperatures are significantly smaller than the associated variations in upland-lowland soil moisture.

5.2.3. Coupling soil decomposition and NPP: The nitrogen cycle. The products of soil decomposition are altered organic material, CO_2 and mineralized nitrogen. On an annual basis, net nitrogen mineralization in tussock tundra is ~0.1-0.3 g N m^{-2} yr^{-1} [*Shaver et al.*, 1991]. This rate is not sufficient to meet the annual plant uptake requirement of 0.3-0.5 g N m^{-2} yr^{-1} [*Shaver et al.*, 1991] suggesting that mycorrhizal uptake of nutrients [*Bowen and Smith*, 1981] or the direct plant uptake of amino acids [*Kielland*, 1994] are important in this system. This high demand for nitrogen maintains nitrogen concentrations in the soil water at low levels (0.02 g N m^{-2} inorganic nitrogen and 0.04 g N m^{-2} for total dissolved nitrogen) and thus limits the loss of nitrogen from the ecosystem [*Giblin et al.*, 1991; *Shaver et al.*, 1991]. On longer timescales, or during periods of unusually high nitrogen mineralization, more possibilities exist; the C/N ratio of the plants and soils may decrease, nitrogen may be fixed in clays, or as recently suggested by *Lipson et al.* [1996], vegetation may take up nitrogen and store it in proteins to be used at a later date. Tundra plants rely heavily on retranslocated nitrogen to meet their annual nitrogen requirements [*Chapin et al.*, 1978, 1980] and fertilization studies have shown that stored nitrogen reserves increase when nitrogen is added [*Chapin and Shaver*, 1996]. Fertilized tundra plants also accumulate nitrogen more efficiently than agricultural crops because they are strongly nutrient limited [*Chapin et al.*, 1995]. The strong nutrient limitation, as well as the multiplicity of nitrogen storage mechanisms, may explain why the ecosystem strongly retains mineralized nitrogen and why we find the residence time of labile nitrogen is of the order of decades (see section 6.2.2). For this study, we did not specify individual nitrogen fractions but rather used a single "labile" nitrogen fraction which we define to be all forms of mineralized nitrogen resulting from gross decomposition of organic matter that can at present or at a later date be used to meet photosynthetic demands.

A single ecosystem C/N ratio is assumed; that is, all three carbon pools, and the vegetation, have identical C/N ratios. We fully acknowledge that there is a large range in C/N ratios for the pools we model. However, because the mass weighted C/N of the organic material released by soil decomposition is similar to the C/N ratio of the incoming plant material, results would be the same whether we assumed constant or variable C/N for the soil organic

matter pools. This modeling study shows that on average, 40% of the annual soil respiration is from the litter pool, 40% is from the fast pool, and 20% is from the slow pool. Assuming actual C/N ratios for the herbaceous, fast and slow pools to be 50, 25, and 15, respectively, then the mass-weighted C/N ratio of the entire soil column is 33, approximately the C/N ratio of the vegetation [*McKane et al.*, 1997b; *Waelbroeck and Louis*, 1995]. Our implicit assumption is that during the course of our warming simulations, there is no shift in species composition, for example, from a community dominated by tussocks (low C/N) to one dominated by more woody species (high C/N). To account for changes in community composition, our assumption of a single ecosystem C/N ratio would clearly have to be modified and more complex nitrogen dynamics added.

The input of nitrogen to the ecosystem via precipitation throughout the year (rainwater plus snowfall), 0.02 - 0.06 g N m^{-2} yr^{-1}, is approximately equal to the loss of nitrogen in the stream system [*Shaver et al.*, 1991]. On an annual basis we add 0.06 g N m^{-2} to account for the nitrogen entering the system via precipitation. In any case, nitrogen input is insignificant compared to plant growth requirements of ~2-3 g N m^{-2} yr^{-1} [*Chapin et al.*, 1995].

Because the ecosystem residence time of labile nitrogen is considerably longer than either the timescale for snowmelt or storm systems and the fact that not all labile nitrogen may be in dissolved form, the physical export of nitrogen from the ecosystem via base flow is not modeled. Instead, we include a continuous loss of labile nitrogen at a rate proportional to its pool size. The calculation of residence time is described in section 6.2.2.

Finally, biomass harvests in 1983 and 1989 [*Chapin et al.*, 1995; *Shaver and Chapin*, 1991] indicated that 79% of annual NPP was allocated to above ground production, with the remainder contributing to root production. We distribute NPP biomass accordingly; 79% of the annual NPP supplies the surface herbaceous pool, and the remainder supplies the fast pool.

5.2.4. Ecosystem acclimation. *Vourlitis and Oechel* [1999] proposed that the recent return of the system to sink activity may in part be due to ecosystem acclimation. This acclimation may include alterations in leaf nitrogen and LAI and changes in biomass allocation among plant tissues, possibly leading to a shift in community composition. As will be shown in section 6.3.3, the degree of acclimation will play a large role in governing the variability of ecosystem fluxes at intermediate to long timescales. With this in mind, the nutrient manipulation experiments conducted at the Toolik Lake LTER are especially informative.

Since 1980, experimental tussock tundra plots have been fertilized at a rate of 10 g N m^{-2} yr^{-1}. Biomass harvests were conducted during 1983 and 1989 [*Chapin and Shaver*, 1996; *Chapin et al.*, 1995]. In control plots, vascular plants plus moss NPP averaged 120 g C m^{-2} yr^{-1}, while at the fertilized plots, NPP averaged 219 g C m^{-2} yr^{-1}. With the additional inputs of nitrogen, the plants showed an increase in leaf biomass (LAI was not directly measured). In 1983, NPP allocation to leaves was 39 g C m^{-2} yr^{-1} in the control plots and 72 g C m^{-2} yr^{-1} in the fertilized plots. In 1989, allocation to leaves was 22 g C m^{-2} yr^{-1} in control plots and 47 g C m^{-2} yr^{-1} in fertilized plots [*Chapin and Shaver*, 1996]. The amount of nitrogen held above ground also increased considerably with fertilization, 180% by 1983 and nearly 250% by 1989, but there were only modest increases in the percent nitrogen of leaf tissue [*Chapin et al.*, 1995]. This suggests that increased nitrogen availability does not disrupt the LAI-nitrogen relationship used in ACM.

In addition to changes in total biomass and NPP, 9 years of fertilization led to an overall shift in the species composition from graminoids and mosses (low C/N ratio) toward woody plants (high C/N ratio) such as birch [*Chapin et al.*, 1995]. This level of ecosystem response is clearly not taken into account by our model. Therefore if increased nitrogen availability leads to vegetation with a higher C/N ratio than the original community (see discussion by *Shaver et al.* [1991]), predictions we make about net ecosystem carbon balance will be biased toward higher than actual carbon losses.

A soil nitrogen increase of 10 g N m^{-2} yr^{-1} is clearly above any fertilization that would result from a conceivable climate warming, and therefore, these results should be seen as an end-member response of the ecosystem. Another appraisal of the expected ecosystem response to climate warming may be gained from tracer level additions of nutrients. The ^{15}N experiments by *Nadelhoffer et al.* [1999] and L. Johnson et al. (unpublished manuscript, 2000) demonstrate the limited ability of plants to take up labile soil nitrogen on short time scales. From analysis of a single application of ^{15}N at tracer levels to plots at Toolik Lake, L. Johnson et al. (unpublished manuscript, 2000) found that plants had taken up only 2% of the ^{15}N by year one, 10% by year two, and after 6 years, the plant ^{15}N had diminished significantly. However, after 1 week of fertilization, microbes accounted for over 60% of the ^{15}N uptake. These results indicate that the effects of fertilization brought on by warming will first be seen at the microbial level. We propose that increased fertilization will lead to an increase in microbial activity, resulting in a long-term increase in mineralization rates, albeit at a rate slower than the net decomposition rate of organic matter. Through rapid uptake and slow release of nutrients, microbes therefore buffer the system from the impact of large pulses of nitrogen.

Results from two fertilization experiments have been presented; a continuous fertilization at extremely high nitrogen levels and a short-term application at tracer levels. How will the ecosystem respond to continuous fertilization, brought about by soil warming but at tracer levels? This will now be explored by way of a climate warming simulation. Labile nitrogen released to the soil, a by-product of the microbial decomposition of organic matter, will be allowed to remain in the ecosystem for prolonged periods. Leaf nitrogen and LAI will be adjusted according to soil nutrient conditions.

6. Results

6.1. Validation of Hydrologic and Thermal Processes (1991 - 1993)

As stated earlier, meteorological and hydrological data taken at Imnavait Creek from May 1991 through October 1993 were used to force the land surface model. An extensive discussion of model results is found in *Stieglitz et al.* [1999] and will be described briefly here. Figure 4a – 4f shows monthly averages of various watershed water balance components for the period June 1991 through September 1993. With freezing of the soil column beginning in early fall, soil moisture does not change significantly until the onset of spring melt. As the pack ablates in late May and early June, melt waters infiltrate the still frozen ground. The soil is recharged, and the mean water table depth rises from the previous summer value nearly to the surface. The associated partial contributing area increases from 20 to almost 40% (in good

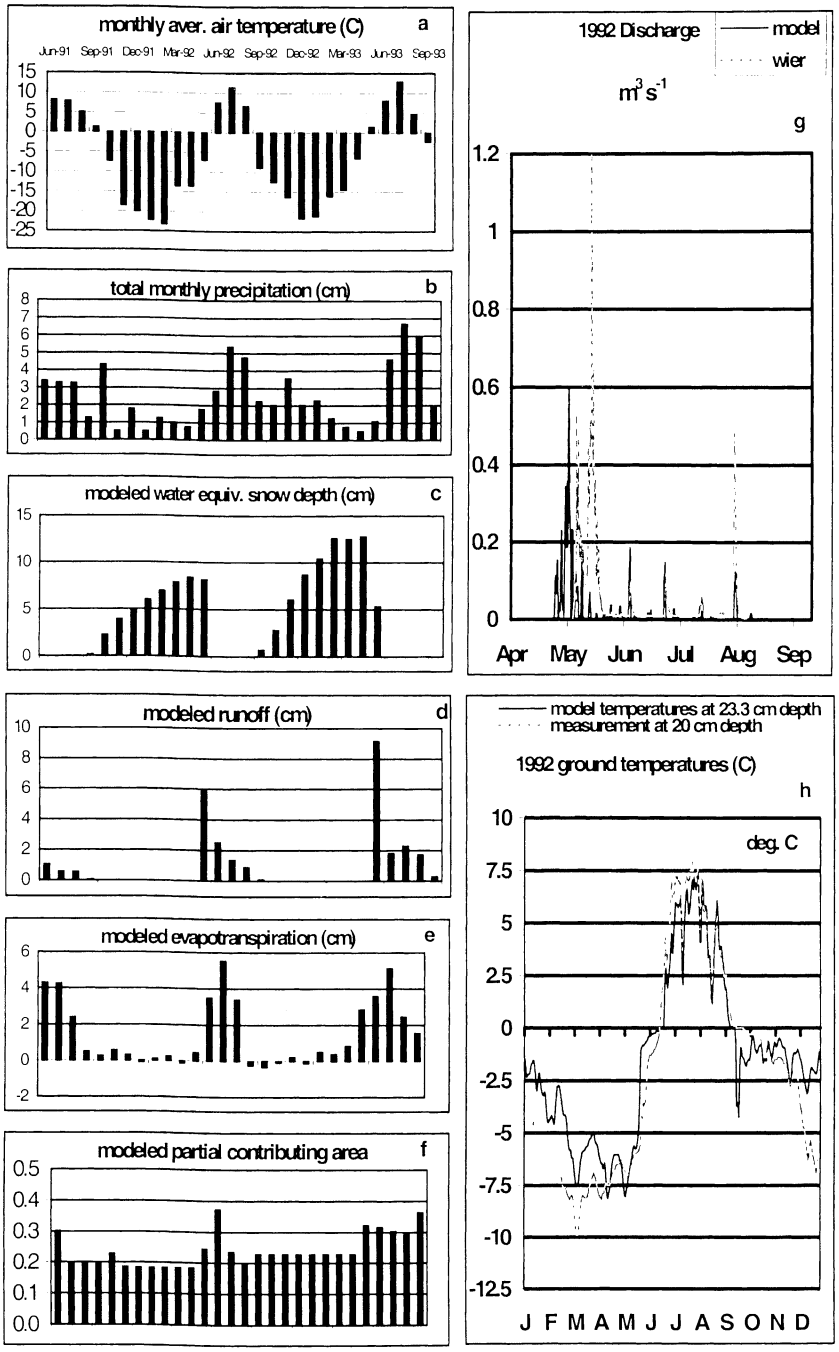

Figure 4. (a) – (f) Modeled monthly averages of various watershed water balance components for the period June 1991 through September 1993. (g) Model-simulated daily runoff and observed runoff measured at the Imnavait Creek weir for the period of April through October 1992. (h) Model-simulated daily averaged ground temperatures and ground temperature data observed at Imnavait Creek during 1992.

agreement with *McNamara et al.* [1997]). Surface runoff generated over the rapidly expanding saturated regions quickly enters the stream system. As the soil active layer deepens in the summer, evapotranspiration (and the latent heat flux) begins to increase, peaks in July and August, and falls rapidly as the snow season approaches. Finally, annual precipitation is partitioned 47% into runoff and 53% into evapotranspiration; this is the partitioning measured in the long-term field record. Modeled ground temperatures are in good agreement with measurements (Figure 4h).

Overall, both the spring hydrographs resulting from the collapse of the winter snowpack and the summer storm hydrographs are reasonably simulated (Figure 4g). However, a current deficiency with the hydrologic simulation is that snow heterogeneity impacts the timing and quantity of snowmelt related discharge. Because the spatial distribution of snow cover is not represented

in the model framework, modeled snowmelt consistently leads actual snowmelt by 5-10 days. With high winds and low vegetation height, snow in this region of the Arctic tends to blow into valleys and build up [*Kane et al.*, 1991; *Liston*, 1986; *Liston and Sturm*, 1998]. As such, it takes longer to melt a snowpack whose depth is substantially increased over a reduced area compared to a pack that is uniformly distributed over the landscape. Further, *Hinzman et al.* [1996] point out that the thick and dense snowpack on the valley floor functions as a dam; it holds back the water until the bonding strength of the snow is overcome.

The impact of this 5 to 10 day error in snowpack ablation on the subsequent simulations is small. The remaining simulations are comparative in nature; that is we explore how a climate change scenario impacts the trend in such measures as the number of snow-free days, microbial respiration, NPP, and the variability in CO_2 fluxes. Therefore while the determination of the model parameters (section 6.2) will be somewhat impacted, conclusions with respect to climate change and trends should be robust.

6.2. Determining Model Parameters

The land surface model was forced with our constructed meteorological data set from 1900 to 1940. For our initial calibrations, we assume net ecosystem productivity (NEP; NEP is NPP minus soil respiration and is positive when terrestrial carbon is accumulating) during the early part of the 20th century was in sum zero. That is, the terrestrial biosphere was neither a net sink nor source of carbon to the atmosphere. This assumption is both consistent with modeling studies by *McKane et al.* [1997b] at Toolik Lake, and the observation that soil respiration generated by the model shows no long-term trend during this period.

6.2.1. Microbial decomposition constants, K_j, and ACM parameters. NPP measurements at Toolik Lake in 1983 and 1989 averaged 120 g C m^{-2} yr^{-1} [*Chapin et al.*, 1995; *Shaver and Chapin*, 1991]. Assuming that over the period 1900 - 1940, NEP is zero, and using an average NPP of 120 g C m^{-2} yr^{-1}, we solve for the annual soil carbon fluxes from each of the three soil pools (Figure 2b). The land surface model is then forced with our constructed meteorological data set from 1900 to 1940 to determine those K_j values that satisfy these soil fluxes on an annual basis. We calculate turnover times of 0.5, 21, and 664 years for the herbaceous, fast, and slow pool, respectively (Figure 2b).

The ^{14}C data from another northern site with peat soils, the BOREAS northern site [*Trumbore and Harden*, 1997], yield turnover times for surface detritus ranging from 6 years in well-drained uplands to 250 years in wetlands. Deep soil carbon turnover ranged from 100 years to greater than 3000 years, again primarily depending on the long-term status of soil moisture. As shown in Figure 4f, the annual mean partial contributing area simulated at Imnavait Creek is 20%. Applying this to BOREAS data, 20% of the deep carbon would have a turnover of ~3000 years while 80% of the deep carbon would have a turnover of ~100 years. This yields a mean watershed turnover of 680 years for the deep carbon pool, in good agreement with the model generated carbon turnover of 664 years for the slow pool (in the model the slow pool accounts for 94% of the total soil carbon pool modeled).

Leaf nitrogen (1.57 g N (m^2 ground area)$^{-1}$) and LAI (0.98 (m^2 leaf area) (m^2 ground area)$^{-1}$) are determined by ACM such that potential NPP over the 40-year simulation averages 120 g C m^{-2} yr^{-1}. These values are a bit higher but in reasonable agreement with site data [*Williams and Rastetter*, 1999]. Our higher values are due to the fact that we are trying to match the total (vascular and nonvascular) site NPP rather than just the vascular component so as to simulate historical levels of whole ecosystem carbon fluxes. We now determine that minimum ecosystem residence time for labile nitrogen such that this potential NPP of 120 g C m^{-2} yr^{-1} equals actualized NPP over the period 1900 - 1940.

6.2.2. Ecosystem residence time of nitrogen. With LAI, leaf nitrogen, and K_j values determined, all that remains is to determine the ecosystem residence time, t_{res}, of labile nitrogen. The equation that governs the dynamics of the labile nitrogen pool is

$$\frac{dN_l}{dt} = I_{dep} - I_{uptake} + I_{min} - N_l e^{-t/tres} \quad (3)$$

where N_l is the labile nitrogen pool size at time t, I_{dep} is the nitrogen entering the system via precipitation, I_{min} is the mineralized nitrogen resulting from microbial decomposition of organic matter, I_{uptake} is the nitrogen uptake by vegetation, and t_{res} is the ecosystem residence time of labile nitrogen. We assume I_{min} represents nitrogen mineralization resulting from gross organic decomposition.

A suite of experiments is conducted in which the land surface model is driven with the 1900 - 1940 hourly forcing data described above. Experiments differ only in the value specified for t_{res} (Figure 5). When $t_{res} = 0$, the plant either uses the available labile nitrogen or it immediately leaks out of the system. This "use it or lose it" scenario results in a large and continual loss of nitrogen and, therefore carbon, from the ecosystem. Annual carbon loss decreases as t_{res} increases until t_{res} = 1.5 decades, when carbon loss is ~ 2 g C m^{-2} yr^{-1}, or considering a soil-plant C/N ratio of 33, equal to the annual nitrogen input from precipitation. Thus the steady state t_{res} is taken to be that residence time such that annual loss of ecosystem nitrogen equals the annual input via precipitation. This 1.5 decade residence time is used for the remainder of the modeling.

6.3. Climate Change (1940 - 2060)

The land surface model is now forced with our constructed meteorological data set from 1940 to 2060. Figures 6a and 6b

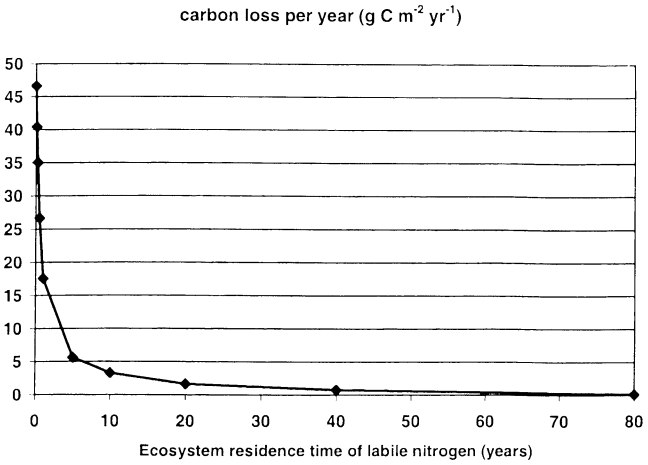

Figure 5. Terrestrial carbon loss per year as a function of the ecosystem residence time for labile nitrogen.

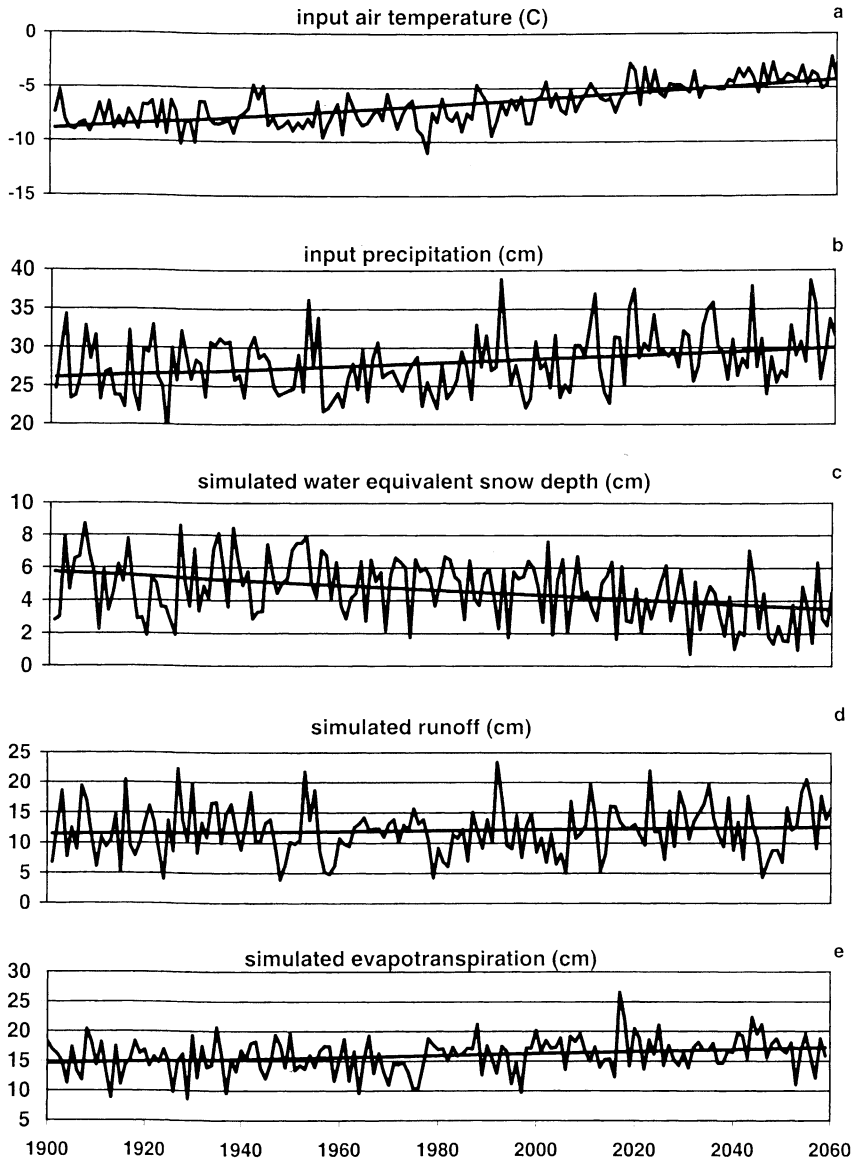

Figure 6. Yearly averaged water balance components. Simulated water equivalent snow depth shown is averaged over a 365-day period. The straight line is the linear trendline.

display the forcing variables, air temperature and precipitation. While the 1990 - 2060 mean annual air temperatures increase by 4°C, most of the warming (3°C) occurs during the long winter months. Nearby ice-free ocean conditions that prevail in summer months act to diminish the overriding warming through evaporative cooling [*Houghton et al.*, 1995]. The decrease in the interannual variability of air temperature seems associated with an enhanced period of ice-free ocean conditions. With higher annual air temperatures, the atmospheric water holding capacity increases and precipitation increases by 10% from 1990 to 2060. As stated earlier, while some GCM simulations do produce slightly more warming, the drying effects of enhanced warming are offset by enhanced precipitation. All simulations, however, yield more winter warming than summer warming, as has been observed [*Chapman and Walsh*, 1993; *Overpeck and al.*, 1997].

Our model indicates that over the period 1940-2060, soil respiration will increase significantly, by 36% (Figure 7b). However, the effect that this increased soil respiration has on ecosystem carbon fluxes is largely determined by the degree to which the plants can respond to the increased nitrogen availability. To explore this we allow total leaf nitrogen g N (m^2 ground area)$^{-1}$ to adjust to increased nitrogen availability. Three scenarios are presented for the period 1940 – 2060: no adjustment to leaf nitrogen, a 20% increase in the leaf nitrogen over the period 1940 - 2060, and finally, a 40% increase over the same period. LAI adjusts according to the LAI-nitrogen relationship discussed in section 5.2.1. Each scenario begins with the same 1900 - 1940 period for which acclimation was not an issue.

6.3.1. Hydrologic processes. Owing to increased winter sublimation and warmer winter temperatures, the number of snow-free days increase from 121 to 157 over the 1990-2060 warming period (Figure 7d). Snow seasons begin later and end earlier, and the seasonal water equivalent snowpack decreases by 43% (Figure

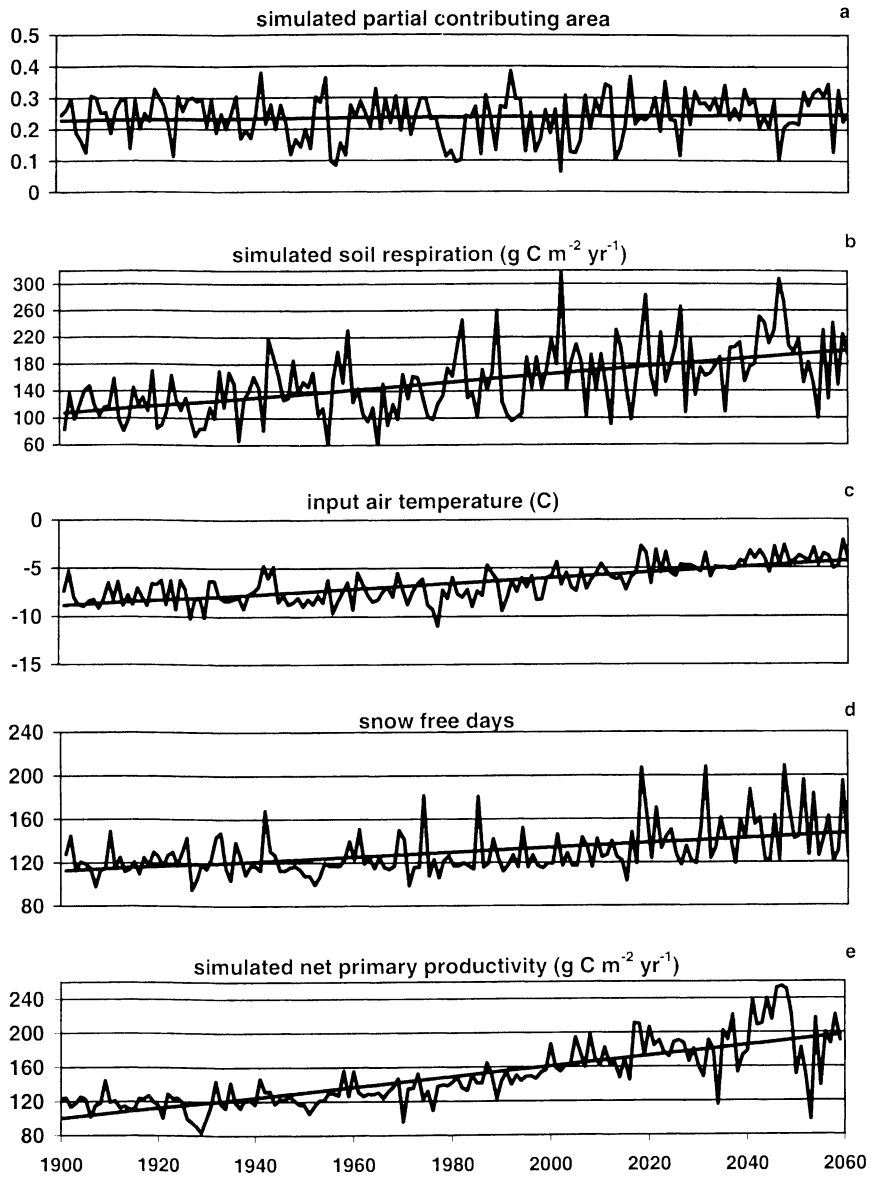

Figure 7. Yearly averaged simulated fields. Correlations show soil respiration is most strongly correlated with the catchment moisture status, and to a lesser extent, surface air temperature, while NPP is most correlated with ambient air temperature and the number of snow-free days. Soil respiration and NPP shown correspond to the scenario in which leaf nitrogen linearly increases by 20% over the period 1940 - 2060. The simulated partial contributing area represents that fraction of the catchment that is saturated. Straight line is the linear trendline.

6c). Runoff and evapotranspiration (Figures 6d and 6e) both increase slightly; however, runoff as a fraction of precipitation remains fairly constant throughout the warming. Mean annual deep ground temperatures warm by 1.25°C while the maximum soil active layer deepens by ~35 cm.

It might intuitively be expected that an overall warming of arctic air temperatures would lead to a diminution of runoff. This does not appear to be the case (Figure 6d). With most of the warming occurring in the long winter months, the impact on annual evapotranspiration (winter sublimation plus summer evapotranspiration) is significantly less than it would otherwise be had the warming been more uniformly distributed throughout the year. Any enhanced annual evapotranspiration is easily accommodated by the associated increase in precipitation. In fact, this model result of increased runoff in the face of an overall warming trend is consistent with observations. From 1930 through 1990, Siberian rivers, specifically, the Lena, Pechora, Yenisey, and the Ob, all have seen an increase in runoff by ~10% [*Lammers et al.*, 2000]. Over the same period, annual air temperatures have increased by ~1-2°C, with a clear bias toward winter warming [*Chapman and Walsh*, 1993; *Overpeck and al.*, 1997], and mean annual precipitation has increased by ~5% (*National Climate Data Center Climate Visualization web site*).

6.3.2. Carbon dynamics operating over short to intermediate timescales. Aggregating hourly model-generated data to annual timescales, the correlation between soil respiration and the

extent of the partial contributing area (Figures 7a and 7b) is found to be -0.58 (significant at the 99% confidence level). When catchment recharge is small, base flow decreases, lowland saturated zones shrink, and the partitioning of anaerobic/aerobic respiration clearly favors the faster aerobic respiration (see (2)). Large effluxes of soil CO_2 are therefore associated with a small partial contributing area. When upland recharge is large, base flow increases, lowland saturated zones expand, and the slower anaerobic respiration plays a bigger role with respect to overall respiration. A smaller release of soil CO_2 is therefore associated with a larger partial contributing area. The correlation between soil respiration and air temperature is somewhat smaller, +0.47 (significant at the 99% confidence level), mostly because ground temperatures, while possibly warmer near the surface, are confined to a relatively cold range at depth. The NPP, however, is highly correlated with air temperature, either directly (+0.76, significant at the 99% confidence level) or indirectly, through a longer growing season (+0.70, significant at the 99% confidence level). NPP is not significantly correlated with the partial contributing area (+0.03) primarily because photosynthesis is for the most part not water-limited in this region. These correlations are highly consistent with results of in situ manipulations of the water table and ambient air temperature at a wet sedge tundra site at Prudhoe Bay, Alaska [*Oechel et al.*, 1998]. In summary, catchment respiration is most strongly correlated with the catchment moisture status and, to a lesser extent, surface air temperature, while NPP is most correlated with ambient air temperature and the number of snow-free days.

The dynamics operating at this short-to-intermediate timescale are best brought out by example. In the early years of the 2040s the partial contributing area is quite small, soil respiration is high (Figures 7a and 7b), and NEP is negative (Figure 8b); the terres-

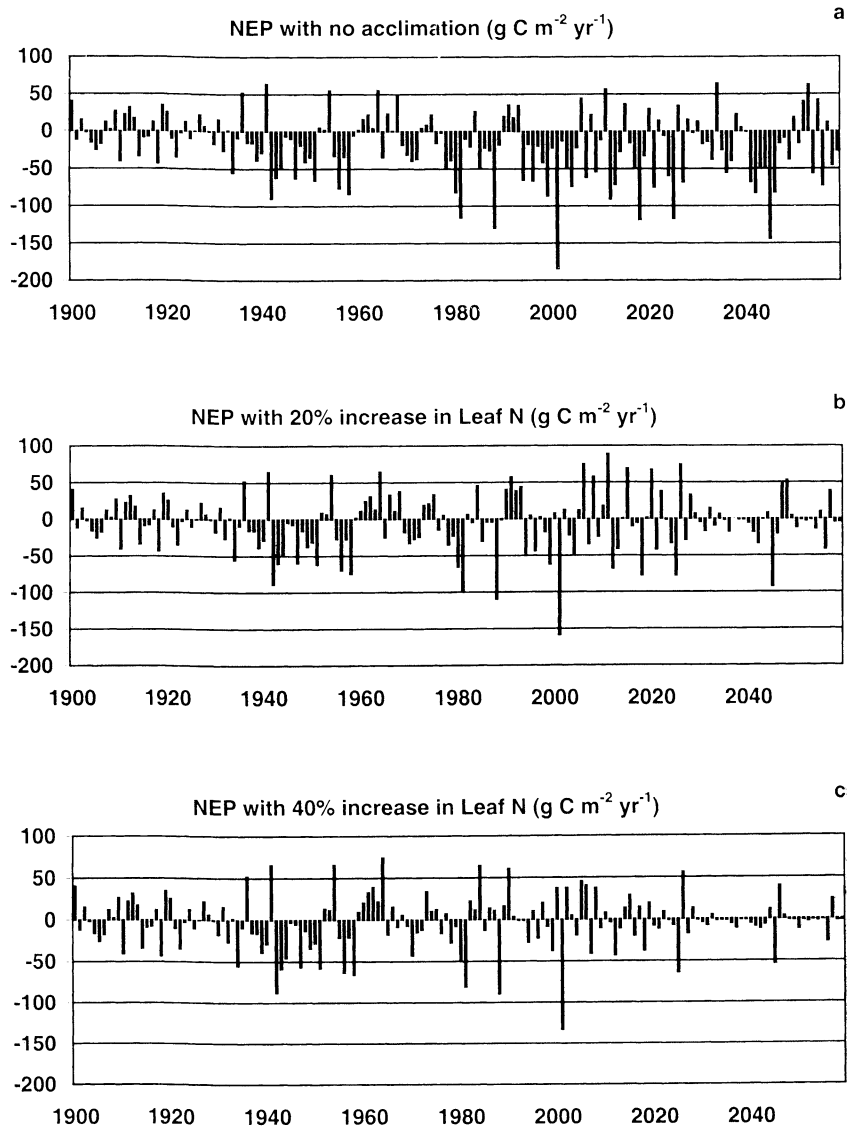

Figure 8. Yearly NEP for the period 1900 - 2060. (a) Leaf nitrogen remains fixed over the entire simulation period. (b) Leaf nitrogen increases linearly by 20% from 1940 to 2060. (c) Leaf nitrogen increases linearly by 40% from 1940 to 2060. For all scenarios LAI adjusts according to the LAI-nitrogen relationship discussed in section 5.2.1. A positive sign reflects terrestrial carbon sequestration.

trial biosphere is losing carbon. As wetter conditions begin to prevail between 2045 and 2055, the partial contributing area expands, and soil respiration markedly decreases. As soil respiration falls below 220 g C m^{-2} yr^{-1}, NPP stays relatively high only because the vegetation is able to make use of nitrogen released to the soil column during the early 2040s. Soil respiration continues to fall, and the continued supply of nitrogen to the soil diminishes until the available soil pool of labile nitrogen is used up and NPP precipitously collapses in the mid 2050s (Figure 7e).

6.3.3. Carbon dynamics operating over intermediate to long timescales: Ecosystem acclimation. For the no acclimation scenario (Figure 8a), soil respiration outstrips potential NPP after 1940, and the terrestrial biosphere more or less continually loses carbon to the atmosphere. The net loss of carbon over the period 1940 - 2060 averages 21.5 g C m^{-2} yr^{-1}, or in total, 16% of the current soil pool. When leaf nitrogen increases by 20% the net loss of carbon averages 4.9 and 0.7 g C m^{-2} yr^{-1} for the periods 1940 - 2060 and 1990 -2060, respectively (Figure 8b). When leaf nitrogen is allowed to increase by 40%, potential photosynthesis keeps up with increased soil respiration, and the system oscillates between sink and source activity (Figure 8c). The net loss of carbon averages 2.1 and 0.0 g C m^{-2} yr^{-1} for the periods 1940 - 2060 and 1990 -2060, respectively. While the degree of leaf response (increased leaf nitrogen and increased LAI) clearly impacts the overall simulation, additional insight can be gained by examining the years 1940 - 1960. The period 1940 - 1955 is characterized by a prolonged diminution in the partial contributing area and an associated increase in soil respiration (Figure 7). For the three scenarios described, none incorporates sufficient adaptation to significantly diminish the net loss of carbon to the atmosphere. However, when conditions favorable to carbon sequestration return in the late 1950s, the scenario showing the greatest leaf response also shows the strongest carbon sink activity. Here we see the interaction between acclimation and the ecosystem residence time for labile nitrogen. Nitrogen released during an earlier period is to a large degree retained within the ecosystem to be used at a later date. When conditions favoring carbon sequestration return, those ecosystems showing the greatest degree of acclimation will make most immediate use of this retained nitrogen.

How will this ecosystem respond to the potential nitrogen fertilization brought about by soil warming and increased soil decomposition? Long-term manipulation experiments at the Toolik Lake LTER indicate that the "no response" case is unrealistic for strongly nutrient limited systems such as tundra. However, ^{15}N additions by L. Johnson et al. (unpublished manuscript, 2000) indicate that extremely high plant response is also unrealistic, as effects of fertilization will be seen first at the microbial level. An intermediate response is most probable, but until more long-term manipulations are conducted, this may remain uncertain. However, an increase of 20% in leaf nitrogen is modest compared to increases observed for the long-term, high nitrogen level manipulations at Toolik Lake. Further, if there is a shift toward more woody species, even the small net loss of terrestrial carbon for the intermediate adaptation scenario could be considered a lower limit.

7. Conclusion

Three mechanisms have been identified, each operating at a different timescale, that may govern carbon dynamics in arctic tundra regions and partially explain the variability of observed CO_2 fluxes. At short timescales the biosphere reacts to meteorological forcing. Drier conditions are associated with aerobic soil decomposition, a large CO_2 efflux, and negative NEP. Cooler and moister conditions favor slower anaerobic decomposition, good growing conditions, and positive NEP. At intermediate timescales, periods of terrestrial carbon loss are directly linked to periods of carbon sequestration by the ability of the ecosystem to retain labile nitrogen. Labile nitrogen released to the soil during periods of source activity (soil respiration > net primary productivity) is retained within the ecosystem and accessed during periods when carbon sequestration is favored (net primary productivity > soil respiration). Finally, modulating these dynamics at intermediate to long timescales is the ability of vegetation to respond to long-term changes in soil nutrient status via changes in leaf nitrogen and LAI. A fourth mechanism, not explored in this study, involves a change in carbon allocation, possibly resulting from a change in the community composition which would alter the C/N ratio of living biomass.

Climate warming simulations indicate the following: (1) Except for a longer growing season and a smaller seasonal snowpack, the overall hydrologic cycle is not significantly altered by the future climate warming. (2) The model reproduces realistic variability in ecosystem carbon fluxes only if the ability to retain labile nitrogen over prolonged periods of time is included. (3) Changes in ecosystem CO_2 fluxes brought on by climate variability are strongly buffered by labile nitrogen retention over prolonged periods as well as by the response of vegetation to soil nutrient conditions. (4) For the warming scenario outlined, the magnitude and sign of the net ecosystem carbon exchange will depend primarily on the degree to which the ecosystem acclimates to changing soil nutrient conditions.

This work has implications for the analysis of the recent record of CO_2 fluxes. If we accept that the ecosystem residence time for labile nitrogen is of the order of decades, then the memory of nitrogen in the system is also of the order of decades. The current CO_2 flux database spans a period of 25 years or so, comparable to the ecosystem residence time of labile nitrogen. As such, the current database covers too short a timescale to conclude anything about the impact of climate change on net ecosystem carbon balance. Until such time that the flux database is significantly longer or that our understanding of the behavior of the labile nitrogen pool is significantly better, we will not be able to say with certainty if the arctic tundra will be a source or sink of carbon in a warmer climate. Modeling therefore remains an important tool to better understand how climate, topography, soils, and vegetation will interact to affect the long-term carbon balance of arctic ecosystems.

Acknowledgments. This research was supported by NSF grants from the division of Environmental Biology (Arctic LTER Project), from the office of Polar Programs (Arctic Natural Sciences, Arctic Systems Science (Land-Atmosphere-Ice-Interactions)), and by a NOAA Global Change fellowship. We thank Doug Kane and Larry Hinzman at the University of Alaska, Fairbanks, for generously supplying the data sets used in this study. We also thank Loretta Johnson for supplying unpublished ^{15}N data.

References

Beltrami, H., and J. C. Mareschal, Recent warming in eastern Canada inferred from geothermal measurements, *Geophys. Res. Lett.*, *18*(4), 605-608, 1991.

Beven, K. J., Hillslope runoff processes and flood frequency characteristics, in *Hillslope Processes*, edited by A. D. Abrahams, pp. 187-202, Allen and Unwin, Winchester, Mass., 1986a.

Beven, K. J., Runoff production and flood frequency in catchments of order *n*: An alternative approach, in *Scale Problems in Hydrology*, edited by V.K. Gupta, I. Rodriguez-Iturbe, and E.F. Wood, pp. 107-131, D. Reidel, Norwell, Mass., 1986b.

Beven, K. J., and M. J. Kirkby, A physically-based variable contributing area model of basin hydrology, *Hydrol. Sci. J*, *24*(1), 43-69, 1979.

Beven, K., P. Quinn, R. Romanowicz, J. Freer, J. Fisher, and R. Lamb, TOPMODEL and GRIDATB, A users guide to the distribution versions (94.01), Cent. for Res. on Environ. Syst. and Stat., Lancaster Univ., Lancaster, England., U.K.,1994.

Billings, W. D., Carbon balance of Alaskan tundra and taiga ecosystems: Past, present, and future, *Quat. Sci. Rev.*, *6*, 165-177, 1987.

Bowen, G. D., and S. E. Smith, The effects of mycorrhizas on nitrogen uptake by plants., in *Terrestrial Nitrogen Cycles*, edited by F.E. Clark and T. Rosswall, pp. 237-247, Swed. Nat. Sci. Res. Counc., Stockholm, 1981.

Chapin, F. S., III, R. J. Barsdate, and D. Barel, Phosphorus cycling in Alaskan coastal tundra: A hypothesis for the regulation of nutrient cycling, *Oikos*, *31*, 189-199, 1978.

Chapin, F. S., and G. R. Shaver, Physiological and growth responses of arctic plants to a field experiment simulating climatic change, *Ecology*, *77*(3), 822-840, 1996.

Chapin, F. S., III., P. C. Miller, W. D. Billings, and P. I. Coyne, Carbon and nutrient budgets and their control in coastal tundra, in *An Arctic Ecosystem: The Coastal Tundra at Barrow, Alaska*, edited by J. Brown et. al., pp. 236-265, Van Norstrand Reinhold, New York, 1980.

Chapin, F. S., G. R. Shaver, A. E. Giblin, K. J. Nadelhoffer, and J. A. Laundre, Responses of arctic tundra to experimental and observed changes in climate, *Ecology*, *76*(3), 694-711, 1995.

Chapman, W. L., and J. E. Walsh, Recent variations of sea ice and air-temperature in high-latitudes, *Bull. Am. Meteorol. Soc.*, *74*(1), 33-47, 1993.

Coyne, P. I., and J. J. Kelley, CO_2 exchange over the Alaskan arctic tundra: Meteorological assessment by an aerodynamic method, *J. Applied Ecol.*, *12*, 587-611, 1975.

Dixon, R. K., S. Brown, R. A. Houghton, A. M. Solomon, M. C. Trexler, and J. Wisniewski, Carbon pools and flux of global forest ecosystems, *Science*, *263*(5144), 185 -190, 1994.

Ducharne, A., R. D. Koster, M. J. Suarez, M. Stieglitz, and P. Kumar, A catchment-based approach to modeling land surface processes, 2, Parameter estimation and model demonstration, *J. Geophys. Res.*, in press, 2000.

Field, C., and H. A. Mooney, The photosynthesis-nitrogen relationship in wild plants, in *On the Economy of Plant Form and Function*, edited by T. J. Givnish, pp. 25-55, Cambridge Univ. Press, New York, 1986.

Garfinkel, H. L., and L. Brubaker, Modern climate-tree-growth relationships and climatic reconstruction in sub-arctic Alaska, *Nature*, *286*, 872-873, 1980.

Giblin, A. E., K. J. Nadelhoffer, G. R. Shaver, J. A. Laundre, and A. J. McKerrow, Biogeochemical diversity along a riverside toposequence in arctic Alaska, *Ecol. Monogr.*, *61*(4), 415-435, 1991.

Gorham, E., Northern peatlands - Role in the carbon-cycle and probable responses to climatic warming, *Ecol. Appl.*, *1*(2), 182-195, 1991.

Haugen, R. K., S. I. Outcalt, and J. C. Harle, Relationships between estimated mean annual air and permafrost temperatures in North Central Alaksa, paper presented at *Permafrost-Fourth International Conference,* Natl. Acad. of Sci., Washington, D.C., 1982.

Hinzman, L. D., D. L. Kane, R. E. Gieck, and K. R. Everett, Hydrologic and thermal-properties of the active layer in the Alaskan Arctic, *Cold Reg. Sci. Technol.*, *19*(2), 95-110, 1991.

Hinzman, L. D., D. L. Kane, C. S. Benson, and K. R. Everett, Energy balance and hydrological processes in an arctic watershed, in *Landscape Function and Disturbance in Arctic Tundra*, edited by J. F. Reynolds, and J. D. Tenhunen, pp. 131-154, Springer-Verlag, New York, 1996.

Houghton, J. T., et al. (Eds.), *Climate Change 1995: The Science of Climate Change*, Cambridge Univ. Press, New York, 1995.

Jacoby, G. C., and R. D. Darrigo, Tree-ring width and density evidence of climatic and potential forest change in Alaska, *Global Biogeochem. Cycles*, *9*(2), 227-234, 1995.

Kakuta, S., Surface-temperature history during the last 1000 years near Prudhoe Bay, Alaska - Applying control-theory to the inversion of borehole temperature profiles, *Global Planet. Change*, *98*(2-4), 225-244, 1992.

Kane, D. L., L. D. Hinzman, C. S. Benson, and G. E. Liston, Snow hydrology of a headwater arctic basin, 1, Physical measurements and process studies, *Water Resour. Res.*, *27*(6), 1099-1109, 1991.

Kielland, K., Amino acid absorption by arctic plants: Implications for plant nutrition and nitrogen cycling, *Ecology*, *75*, 2372-2383, 1994.

Lachenbruch, A. H., and B. V. Marshall, Changing climate: geothermal evidence from permafrost in the Alaskan Arctic, *Science*, *234*(4777), 689-696, 1986.

Lammers, R. B., A. I. Shiklomanov, C. J. Vörösmarty, B. M. Fekete, and B. J. Peterson, Assessment of contemporary arctic river runoff based on observational discharge records, *J. Geophys. Res.*, in press, 2000.

Lipson, D. A., W. D. Bowman, and R. K. Monson, Luxury uptake and storage of nitrogen in the rhizomatous alpine herb, Bistorta bistortoides, *Ecology*, *77*(4), 1277-1285, 1996.

Liston, G. E., Seasonal snowcover of the foothills region of Alaska's arctic slope: A survey of properties and processes, M.S. thesis, Univ. of Alaska, Fairbanks, 1986.

Liston, G. E., and M. Sturm, A snow-transport model for complex terrain, *J. Glaciol.*, *44*(148), 498-516, 1998.

Lynch-Stieglitz, M., The development and validation of a simple snow model for the GISS GCM, *J. Clim.*, *7*(12), 1842-1855, 1994.

McKane, R. B., E. B. Rastetter, G. R. Shaver, K. J. Nadelhoffer, A. E. Giblin, J. A. Laundre, and F. S. Chapin, Climatic effects on tundra carbon storage inferred from experimental data and a model, *Ecology*, *78*(4), 1170-1187, 1997a.

McKane, R. B., E. B. Rastetter, G. R. Shaver, K. J. Nadelhoffer, A. E. Giblin, J. A. Laundre, and F. S. Chapin, Reconstruction and analysis of historical changes in carbon storage in arctic tundra, *Ecology*, *78*(4), 1188-1198, 1997b.

McNamara, J. P., D. L. Kane, and L. D. Hinzman, Hydrograph separations in an Arctic watershed using mixing model and graphical techniques, *Water Resour. Res.*, *33*(7), 1707-1719, 1997.

McNamara, J. P., D. L. Kane, and L. D. Hinzman, An analysis of streamflow hydrology in the Kuparuk River Basin, arctic Alaska: A nested watershed approach, *J. Hydrol.*, *206*(1-2), 39-57, 1998.

Miller, P. C., R. Kendall, and W. C. Oechel, Simulating carbon accumulation in northern ecosystems, *Simulation*, *40*, 119-131, 1983.

Nadelhoffer, K. J., B. A. Emmett, P. Gundersen, O. J. Kjonaas, C. J. Koopmans, P. Schleppi, A. Tietema, and R. F. Wright, Nitrogen deposition makes a minor contribution to carbon sequestration in temperate forests, *Nature*, *398*(6723), 145-148, 1999.

Oechel, W., and W. D. Billings, Effects of global warming on the carbon balance of arctic plants and ecosystems, in *Arctic Ecosystems in a Changing Climate: An Ecophysiological Perspective*, edited by F. S. Chapin et al., pp. 139-168, Academic, San Diego, Calif., 1992.

Oechel, W. C., S. J. Hastings, G. Vourlitis, M. Jenkins, G. Riechers, and N. Grulke, Recent change of arctic tundra ecosystems from a net carbon-dioxide sink to a source, *Nature*, *361*(6412), 520-523, 1993.

Oechel, W. C., A. C. Cook, S. J. Hastings, and G. L. Vourlitis, Effects of CO_2 and climate change on arctic ecosystems, in *British Ecological Society Conference on Arctic Ecosystems*, edited by S. Woodin and .M. Marquiss, pp. 255-273, Blackwell Sci., Malden, Mass., 1995.

Oechel, W. C., G. Vourlitis, and S. J. Hastings, Cold season CO_2 emission from arctic soils, *Global Biogeochem. Cycles*, *11*(2), 163-172, 1997.

Oechel, W. C., G. L. Vourlitis, S. J. Hastings, R. P. Ault, and P. Bryant, The effects of water table manipulation and elevated temperature on the net CO_2 flux of wet sedge tundra ecosystems, *Global Change Biol.*, *4*(1), 77-90, 1998.

Overpeck, J., et. al., Arctic environmental change of the last four centuries, *Science*, *278*(5341), 1251-1256, 1997.

Pitman, A. J., Z.-L. Yang, J. G. Cogley, and A. Henderson-Sellers, Description of bare essentials of surface transfer for the Bureau of Meteorological Research Centre AGCM, Bur. Meteorol. Res. Cent., Australia, 1991.

Post, W. M., W. R. Emanuel, P. J. Zinke, and A. G. Strangenberber, Soil carbon pools and world life zones, *Nature*, *298*(5870), 156-159, 1982.

Schlesinger, W. H., Carbon balance in terrestrial detritus, *Annu. Rev. of Ecol. Syst.*, *8*, 51-81, 1977.

Shaver, G. R., and F. S. Chapin, Production - Biomass relationships and element cycling in contrasting arctic vegetation types, *Ecol. Monogr.*, *61*(1), 1-31, 1991.

Shaver, G. R., K. J. Nadelhoffer, and A. E. Giblin, Biogeochemical diver-

sity and element transport in a heterogeneous landscape, the North Slope of Alaska, in *Quantitative Methods in Landscape Ecology*, edited by M. G. Turner and R. H. Gardner, pp. 105-125, Springer-Verlag, New York, 1991.

Shaver, G. R., W. D. Billings, F. S. Chapin, A. E. Giblin, K. J. Nadelhoffer, W. C. Oechel, and E. B. Rastetter, Global change and the carbon balance of Arctic ecosystems, *Bioscience*, *42*(6), 433-441, 1992.

Stieglitz, M., D. Rind, J. Famiglietti, and C. Rosenzweig, An efficient approach to modeling the topographic control of surface hydrology for regional and global climate modeling, *J. Clim.*, *10*(1), 118-137, 1997.

Stieglitz, M., J. Hobbie, A. Giblin, and G. Kling, Hydrologic modeling of an arctic tundra watershed: Toward Pan- Arctic predictions, *J. Geophys. Res.*, *104*(D22), 27,507-27,518, 1999.

Trumbore, S. E., and J. W. Harden, Accumulation and turnover of carbon in organic and mineral soils of the BOREAS northern study area, *J. Geophys. Res.*, *102*(D24), 28,817-28,830, 1997.

Vourlitis, G. L., and W. C. Oechel, Landscape-scale CO_2, H_2O vapour and energy flux of moist-wet coastal tundra ecosystems over two growing seasons, *J. Ecol.*, *85*(5), 575-590, 1997.

Vourlitis, G. L., and W. C. Oechel, Eddy covariance measurements of CO_2 and energy fluxes of an Alaskan tussock tundra ecosystem, *Ecology*, *80*(2), 686-701, 1999.

Vourlitis, G. L., W. C. Oechel, J. Verfaillie, A. S. Hope, D. A. Stow, W. Boynton, R. C. Zulueta, and S. J. Hastings, Scaling plot-measurements of CO_2 flux across and arctic tundra landscape, *Eos Trans. AGU*, Fall Meet. Suppl., F262, 1998.

Waelbroeck, C., and J. F. Louis, Sensitivity analysis of a model of CO_2 exchange in tundra ecosystems by the adjoint method, *J. Geophys. Res.*, *100*(D2), 2801-2816, 1995.

Whittaker, R. H., *Communities and Ecosystems*, Macmillan, Indianapolis, Indiana, 1975.

Williams, M., and E. B. Rastetter, Vegetation characteristics and primary productivity along an arctic transect: Implications for scaling-up, *J. Ecol.*, *87*(5), 885-898, 1999.

Williams, M., E. B. Rastetter, D. N. Fernandes, M. L. Goulden, S. C. Wofsy, G. R. Shaver, J. M. Melillo, J. W. Munger, S. M. Fan, and K. J. Nadelhoffer, Modelling the soil-plant-atmosphere continuum in a Quercus-Acer stand at Harvard Forest: The regulation of stomatal conductance by light, nitrogen and soil/plant hydraulic properties, *Plant Cell Environ.*, *19*(8), 911-927, 1996.

Williams, M., E. B. Rastetter, D. N. Fernandes, M. L. Goulden, G. R. Shaver, and L. C. Johnson, Predicting gross primary productivity in terrestrial ecosystems, *Ecol. Appl.*, *7*(3), 882-894, 1997.

Williams, M., W. Eugster, E. B. Rastetter, J. P. McFadden, and F. S. Chapin, The controls on net ecosystem productivity along an arctic transect: A model comparison with flux measurements, *Global Change Biol.*, in press, 2000.

Zimov, S. A., I. P. Semiletov, S. P. Daviodov, Y. V. Voropaev, S. F. Prosyannikov, C. S. Wong, and Y. H. Chan, Wintertime CO_2 emission from soils of Northeastern Siberia, *Arctic*, *46*(3), 197-204, 1993.

Zimov, S. A., S. P. Davidov, Y. V. Voropaev, S. F. Prosiannikov, I. P. Semiletov, M. C. Chapin, and F. S. Chapin, Siberian CO_2 efflux in winter as a CO_2 source and cause of seasonality in atmospheric CO_2, *Clim. Change*, *33*(1), 111-120, 1996.

A. Giblin, J. Hobbie, and M. Williams, Marine Biological Laboratory, The Ecosystems Center, Woods Hole, MA 02543.

G. Kling, Department of Biology, University of Michigan, Ann Arbor, MI 48109.

M. Stieglitz, Lamont-Doherty Earth Observatory of Columbia University, Palisades, NY 10964. (marc@ldeo.columbia.edu)

(Received August 18, 1999; revised June 30, 2000;
accepted August 8, 2000.)